

Intensity Inversion in the Balmer Spectrum of C^{5+}

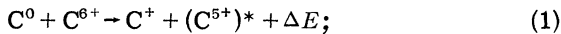
R. H. Dixon, J. F. Seely, and R. C. Elton

Naval Research Laboratory, Washington, D. C. 20375

(Received 22 November 1977)

Intensity inversion between the first ($3 \rightarrow 2$) and second ($4 \rightarrow 2$) Balmer series spectral lines of C^{5+} ions has been observed during plasma expansion into a buffer gas. Numerical modeling indicates that the Balmer spectrum is consistent with the Lyman spectrum and with charge-transfer pumping of the $n = 4$ level. Electron-ion recombination alone is insufficient to explain the observed intensity distribution.

In a recent Letter,¹ it has been suggested that a sudden increase in the Balmer- α line of hydrogenic O^{7+} emitted from a tokamak plasma was the result of the charge transfer reaction $H^0 + O^{8+} \rightarrow H^+ + (O^{7+})^* + \Delta E$, where the asterisk refers to the excited hydrogenic ion formed. However, the observed absence of corresponding increases in the Lyman- α and $-\beta$ lines has made a full interpretation of this experiment difficult. The potential importance of these results to the understanding of charge transfer effects in plasmas has prompted us to measure the complete Balmer spectrum of C^{5+} in a plasma expanding into a buffer gas. Intensity inversion between the Balmer- α and $-\beta$ lines is observed, and inverted population densities are deduced for the $n = 3-6$ levels. Numerical modeling indicates that the $n = 4$ level is pumped by the charge transfer reaction



electron-ion recombination alone is insufficient to explain the intensity inversion. The Balmer spectrum is consistent with the previously reported² Lyman spectrum. We believe this to be the first consolidated report of complete Balmer and Lyman spectra that indicates charge-transfer pumping of excited states of hydrogenic plasma ions.

In this experiment, a Nd-glass laser (5 J, 15 nsec) vaporizes a graphite target, and a plasma containing stripped carbon ions expands into a buffer gas (helium at 1-Torr fill pressure). The highly stripped ions of interest stream outward in a $\sim 20^\circ$ cone normal to the target surface, slowing to a velocity of $\sim 5 \times 10^6$ cm/sec at a distance from the target of ~ 15 mm where they are believed to interact with a neutral carbon cloud. The carbon ion and atom densities at this point are in the range of $10^{13}-10^{14}$ cm⁻³. In this ion-atom interaction zone, an electron temperature of $kT = 1.4 \pm 0.4$ eV has been deduced³ from the

measured ratio of the 2^1P-1^1S resonance and the 2^3P-1^1S intercombination lines⁴ of heliumlike C^{4+} , assuming an equal probability for free-electron capture into the singlet and triplet systems. For the conditions present here, the major triplet population losses are by radiative decay⁵ and by electron spin-exchange collisional transitions to singlet levels. For the latter, a rate⁶ of $1.4 \times 10^{-8} N_e / kT_e$ sec⁻¹ was used (kT in eV) with an electron density $N_e = 5 \times 10^{16}$ cm⁻³ as measured² from Stark-broadened He II lines. This temperature agrees with an extrapolated value from a similar experiment⁷ without a buffer gas, which implies that significant gas cooling of the plasma is not present at a distance of 15 mm.

For the Balmer series measurements, we used a 2.2-m grazing-incidence spectrograph equipped with a gold-coated, 600-groove/mm, 1.5° blaze-angle grating set for an 84.5° angle of incidence.⁸ Forty discharges were required to obtain a useful spectrogram on Kodak SWR emulsion. The results were found to be reproducible, and a typical microdensitometer tracing is shown in Fig. 1. It is immediately noticed that the Balmer- β ($4 \rightarrow 2$) and Balmer- γ ($5 \rightarrow 2$) lines are intense compared to the Balmer- α ($3 \rightarrow 2$) line, which is consistent with the earlier Lyman series results.² Furthermore, the Balmer- β line intensity exceeds that of the Balmer- α line. A numerical model indicates that the relative line intensity distributions of both the Balmer and Lyman spectra are consistent with charge-transfer pumping of the $n = 4$ level. In this model, the evolution of the populations of the n, l sublevels of the hydrogenic ion are calculated for n up to 10. It is essential to calculate the populations of the l states individually, rather than assuming statistical occupation, since radiative decay of the $2p$ state prevents complete electron collisional mixing⁹ with the $2s$ state when $N_e Z^{-6} (kT_e)^{-1/2} < 6 \times 10^{13}$ cm⁻³ eV^{-1/2}, where Z is the nuclear charge.

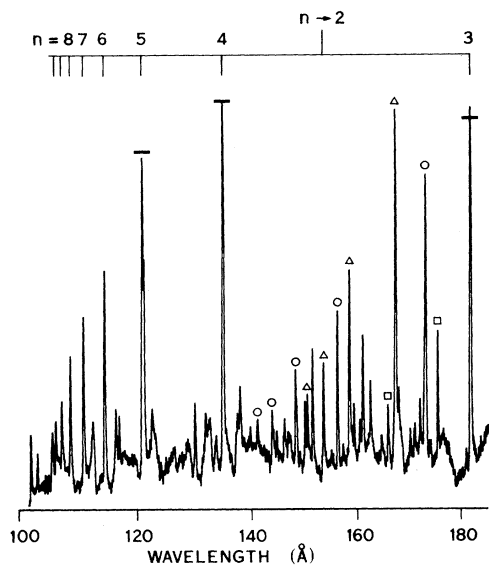


FIG. 1. Microdensitometer tracing of the first-order time-integrated C VI Balmer spectrum (C^{5+} ions) at a distance of 15 mm from the graphite target. The prominent features identified by \square , Δ , and \circ are C V lines (Ref. 4). The horizontal bars indicate relative intensities derived from Lyman series data (Ref. 2) on population densities, assuming a statistical mixing of sublevels.

Processes included in the model are radiative¹⁰ and three-body collisional¹¹ recombination, electron collisional ionization¹¹ and excitation,¹² charge transfer (see below), radiative decay,¹³ and collisional mixing⁹ of the l sublevels for the higher principal quantum numbers n .

The calculated steady state and the experimental Balmer and Lyman spectra are compared in Fig. 2. A best fit to the complete experimental spectra is shown in Fig. 2(a). This calculated result was obtained for the typical collisional scaling parameter $N_e(kT_e)^{-1/2} = (7 \pm 1) \times 10^{16} \text{ cm}^{-3} \text{ eV}^{-1/2}$. The specific numbers chosen for the density and temperature, namely $N_e = 7 \times 10^{16} \text{ cm}^{-3}$ and $kT_e = 1 \text{ eV}$, are within the uncertainties of the experimentally determined values. Also incorporated was a charge-transfer pumping rate $N_a \langle \sigma v \rangle = 5 \times 10^5 \text{ sec}^{-1}$ for capture into the $n = 4$ level of C^{5+} , where N_a refers to the carbon atom density, σ to the charge transfer cross section, and v to the relative ion-atom velocity. For $N_a \approx 10^{14} \text{ cm}^{-3}$ and $v \approx 5 \times 10^6 \text{ cm/sec}$, this corresponds to $\sigma = 10^{-15} \text{ cm}^2$. While partial cross sections have not been calculated for the reaction of

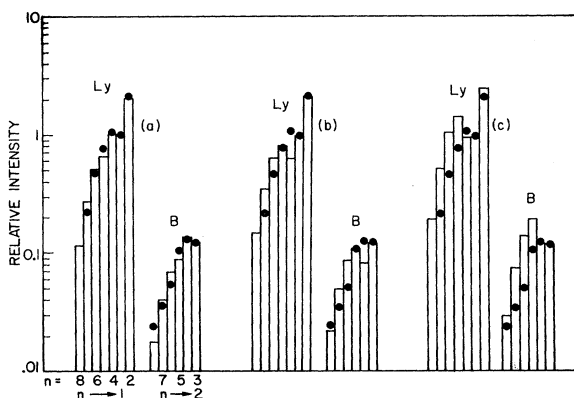


FIG. 2. Calculated (bars) and experimental (dots) relative line intensities for the Lyman (Ly) and Balmer (B) spectra of C^{5+} . All calculated intensities are relative to the Lyman- β line; the experimental spectra are normalized to the calculated $n = 3$ (upper level) line intensities. The intensities were calculated assuming an electron density of $7 \times 10^{16} \text{ cm}^{-3}$, and electron temperatures (kT_e) and charge transfer rates of (a) 1.0 eV, $5 \times 10^5 \text{ sec}^{-1}$, (b) 1.0 eV, 0 sec^{-1} , and (c) 0.1 eV, 0 sec^{-1} , respectively [$kT_e = 0.1 \text{ eV}$ in (c) does not seem realistic, experimentally].

Eq. (1), such a value is consistent with Landau-Zener total-cross-section calculations¹⁴ for the (H, C^{6+}) reaction. We consider the agreement indicated in Fig. 2(a) to be a good fit, with collisional recombination populating high- n states, charge transfer filling intermediate ion states, and cascading and radiative recombination populating the lower- n states.

In Fig. 2(b), only the charge-transfer process has been removed from the model, and the calculated $n = 4$ intensities are seen to fall considerably below the experimental values. Variations of electron temperature and density does not result in improved agreement with the experimental intensities. Inversion of the $n = 3 \rightarrow 2$ and $4 \rightarrow 2$ line intensities occurs in the absence of charge transfer only if $N_e(kT_e)^{-1/2} \gtrsim 2 \times 10^{17} \text{ cm}^{-3} \text{ eV}^{-1/2}$. This condition is shown in Fig. 2(c), where the temperature was reduced to a 0.1-eV extreme. Notice that under these conditions the $n = 4 \rightarrow 2$ and $5 \rightarrow 2$ line intensities are inverted, a phenomenon which has never been observed experimentally. At this low temperature the collision limit drops to the $n = 4$ level, and lower spectral lines are inverted as a result of cascading.

The calculated relative reduced populations (population densities divided by statistical weights) of the n, l states of C^{5+} which generate the spectra of Fig. 2(a) are shown in Fig. 3. Since elec-

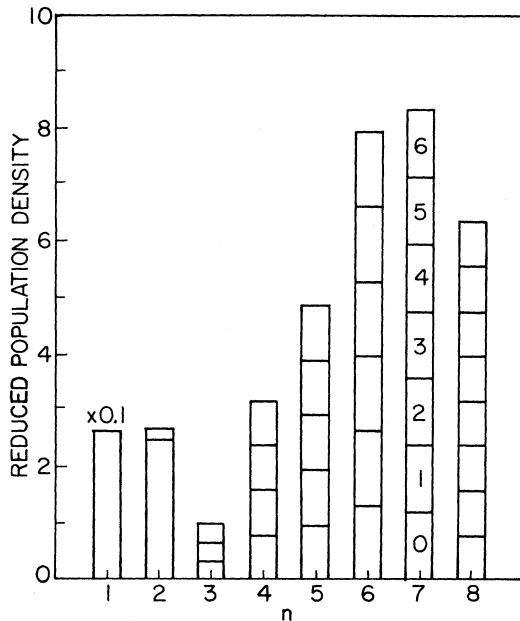


FIG. 3. Relative reduced population densities of the n, l states of C^{5+} calculated as in Fig. 2(a) for an electron temperature $kT_e = 1.0$ eV, an electron density $N_e = 7 \times 10^{16} \text{ cm}^{-3}$, and an $n = 4$ charge transfer rate of $5 \times 10^5 \text{ sec}^{-1}$. The l values progress vertically, as indicated for $n = 7$. Population densities are normalized to the total for the $n = 3$ level. The $n = 1$ population density shown is reduced by a factor of 10.

tron collisional mixing⁹ of l sublevels occurs for $n \geq 3$, reduced populations of such sublevels of a given n level are equal; the population of the $2p$ resonance state is small because of rapid radiative depletion. The populations of levels $n = 3$ through 6 are inverted. Because of the falloff in radiative decay rate with larger n , only the $n = 4$ to 3 population inversion is sufficient to produce an intensity inversion, as observed experimentally.

Of possible concern are opacity effects on the Balmer lines. The optical depth τ of the Balmer- α line may be estimated for Doppler broadening from¹²

$$\tau = 1.1 \times 10^{-16} \lambda N_2 d \bar{f} (\mu/kT_i)^{1/2}, \quad (3)$$

where $\lambda = 182 \text{ \AA}$ is the wavelength,⁴ $\bar{f} = 0.46$ is the absorption oscillator strength¹³ averaged according to relative $n = 2$ populations from Fig. 3(c), $\mu = 12$ is the atomic mass number, $kT_i \geq 1$ eV is the carbon-ion effective temperature, and $d = 0.6$ cm is the depth measured from transverse space-resolved spectra.² From Fig. 3, the population density N_2 of the $n = 2$ absorbing level is approximately an order of magnitude smaller

than that of the ground state of the hydrogenic ion and is therefore $\sim 10^{12} \text{ cm}^{-3}$. This results in an optical depth $\tau \approx 0.02$, indicating an optically thin plasma.

In summary, the newly measured Balmer spectrum is consistent with a numerical model that also agrees with the previously measured Lyman spectrum. Intensity inversions for lines originating on levels 4 and 3 are observed and population inversion for levels 3 through 6 is deduced. The wide range of population inversion results from collisional population and cascading for the higher- n levels, while the intensity inversion and large $n = 4$ to $n = 3$ population inversion requires the selective pumping into $n = 4$ provided by resonance charge transfer.

Valuable discussions with H. R. Griem are recalled with appreciation. This research was supported in part by the U. S. Department of Energy. One of us (J.F.S.) is currently appointed as National Research Council-Naval Research Laboratory Resident Research Associate.

¹R. C. Isler, Phys. Rev. Lett. **38**, 1359 (1977).

²R. H. Dixon and R. C. Elton, Phys. Rev. Lett. **38**, 1072 (1977).

³H.-J. Kunze, A. H. Gabriel, and H. R. Griem, Phys. Fluids **11**, 662 (1968); A. V. Vinogradov, I. Yu. Skobel'ev, and E. A. Yukov, Kvantovaya Elektron. (Moscow) **6**, 1165 (1975) [Sov. J. Quantum Electron. **5**, 630 (1975)].

⁴R. L. Kelly and L. J. Palumbo, *Atomic and Ionic Emission Lines Below 2000 \AA*, U. S. Naval Research Laboratory Report No. 7599 (U.S. GPO, Washington, D. C., 1973).

⁵R. C. Elton, Astrophys. J. **148**, 573 (1967).

⁶A. H. Gabriel and C. Jordan, in *Case Studies in Atomic Collision Physics*, edited by E. W. McDaniel and M. R. C. McDowell (North-Holland, Amsterdam, 1972), Vol. 2, p. 273.

⁷B. C. Boland, F. E. Irons, and R. W. P. McWhirter, J. Phys. B **1**, 1180 (1968); F. E. Irons, R. W. P. McWhirter, and N. J. Peacock, J. Phys. B **5**, 1975 (1972).

⁸The observed intensity inversions are not associated with polarization of the emission since at grazing incidence (and refraction) this grating instrument is not polarization sensitive according to recent data by E. T. Arakawa and M. W. Williams, in Proceedings of the Fifth International Conference on Vacuum Ultraviolet Radiation Physics, Montpellier, France, 1977 (to be published).

⁹H. R. Griem, *Spectral Line Broadening by Plasmas* (Academic, New York, 1974), p. 279, Eq. (526).

¹⁰M. J. Seaton, Mon. Not. Roy. Astron. Soc. **119**, 81 (1959).

¹¹The three-body collisional recombination coefficient

is obtained from the electron collisional ionization coefficient by detailed balancing. The electron collisional ionization coefficient is one half the expression reported by R. W. P. McWhirter, in *Plasma Diagnostic Techniques*, edited by R. H. Huddlestone and S. L. Leonard (Academic, New York, 1965), p. 221, and agrees with a Burgess-Summers semiclassical calculation by M. Blaha (private communication).

¹²R. C. Elton, in *Methods of Experimental Physics, Plasma Physics*, edited by H. R. Griem and R. H. Lovberg (Academic, New York, 1970), Vol. 9A, Chap. 4.

For excitation rates, agreement was found with recent Coulomb-Born distorted-wave calculations by M. Blaha (private communication).

¹³W. J. Karzas and R. Latter, *Astrophys. J. Suppl. Ser.* 6, 167 (1961); W. L. Wiese, M. W. Smith, and B. M. Glennon, *Atomic Transition Probabilities: Hydrogen through Neon*, U. S. National Bureau of Standards Publication No. NSRDS-4 (U.S. GPO, Washington, D. C., 1966), Vol. I.

¹⁴A. Salop and R. E. Olson, *Phys. Rev. A* **13**, 1312 (1976).